



Research paper

Parametric optimization of fillet radius for v6-engin crankshaft under static loading

Hasan Eleashy*

Mechanical Engineering Dept., Faculty of Engineering & Technology, Future University in Egypt, Cairo, 11787, Egypt.

Article info:

Article history:

Received: 00/00/0000

Accepted: 00/00/0018

Revised: 00/00/0000

Online: 00/00/0000

Keywords:

V6-crankshaft,

Fillet radius,

Static analysis,

Simulation,

Parametric optimization.

*Corresponding author:

heashy@fue.edu.eg

Abstract

This paper introduces a new study to improve the performance of a v6-engine crankshaft, as V-type engine crankshaft has little consideration in the literature. First, static analysis for the v6-crankshaft is presented, which includes geometric parameters, loading analysis, and material selection. Secondly, the finite element method is applied to analyze a model for v6-crankshaft with a fine element mesh. The boundary condition is formulated to simulate the proposed model. Then, a solution for maximum equivalent stress, total deformation, and safety factor is carried out. The solution indicates fillet areas are the most critical sections with the highest stress concentrations. Finally, a parametric optimization technique is performed to detect the optimum values for fillet radii that produce minimum equivalent stress and minimum total deformation. The optimized model is compared with the original model and theoretical calculations. In the optimized model, maximum equivalent stress is reduced by 34.45% with an increase in mass by 0.02%. Geometric optimization of the v6-crankshaft design provides an effective methodology to improve its performance.

1. Introduction

The crankshaft is an essential element in an automotive engine. It transmits the reciprocating motion of the piston to a smooth rotational motion. The reliability of an internal combustion engine is based mainly on the strength of the crankshaft. Stress concentration should be seriously considered under the effect of static and variable loads. Failure problems of crankshafts occur primarily at the rounded transition area from the crank to the journal. It is mainly the journal fillet and crankpin fillet. So, fillet areas need to be strengthened to enhance the service life of the crankshaft. The fillet rolling process provides an effective technique

to improve the behavior of crankshaft fillet areas. The crankshaft fillet and fillet rolling process have recently been investigated by many researchers. The importance of the fillet rolling process has been discussed [1]. The endurance stress increases with the fillet rolling process compared to the un-rolled condition.

The optimum rolling load for the crankshaft design was between 20 and 24kN. The fillet rolling process was modeled in FEA with various machine parameters and real boundary conditions. Calculations were applied and validated by the measurements and tests [2]. Residual stresses produced by the fillet rolling process were investigated [3, 4] to identify its effect on the fatigue process of a ductile cast iron

crankshaft under bending loading. A two-dimensional plane strain finite element analysis (FEA) was also applied to analyze residual and bending stresses near the fillet of a crankshaft. Then, bending fatigue tests were conducted. Factors affecting the fillet rolling process were simulated to enhance the influence of compressive residual stress in crankshaft fillets [5]. Resulted variables of impact angle, impact speed, and impact rotation angle were 45°, 10 m/s, and 4.5°, respectively. FEA was performed on different types of engine crankshafts such as a single cylinder four-stroke engine crankshaft and a diesel engine crankshaft [6, 7] to get the difference in stress level at critical locations. Pressure-volume diagram was used to find the load boundary condition. Dynamic analysis was performed analytically and simulated in ADAMS. It was concluded that stress concentration is significantly initiated in the transition area between the main journal and connecting rod journal, and the crank. The single-cylinder engine crankshaft was investigated to improve fatigue life by changing the crankpin fillet radius and crankpin diameter [8]. The effect of different fillet structures on the safety factor of a marine diesel engine crankshaft was presented [9]. Hence, the most suitable crankshaft fillet structure is a two-way sinking groove fillet with a minimum safety factor of 2.209.

Generally, the working conditions of the crankshaft are complicated due to complicated geometry and variable loads during the working process. Therefore, the stiffness and fatigue strength of the journal should be checked during the crankshaft design. A practical technique was involved to investigate the crankshaft fatigue based on a customized experiment platform [10]. Then, statistical regression analysis of eight commonly used hypothesis distributions was conducted. Failure analysis of single-cylinder diesel engine crankshaft and crankshaft of a motor diesel vehicle was carried out [11, 12]. The failure occurred at the sharp fillet region and the lubrication holes, where the stress concentration was at the highest level. The finite element method (FEM) was applied by ANSYS software for crankshafts of a single-cylinder engine and crankshaft of a four-cylinder engine [13, 14]. Both crankshafts were modeled and compared in terms of stress and deformation to

optimize the of crankshaft geometry and safe design.

Dynamic and modal analysis on crankshaft was introduced [15-17] for L-twin cylinder and diesel. Crankshaft dynamic analysis showed that the design of the statically safe crankshaft may fail under the dynamic loading condition of the crankshaft. Maximum deformation and stress appeared at the web edge of the counterweight and maximum stress intensity was initiated at the fillets between crankshaft journal and crankpin. A large amplitude was applied to prevent resonance. The maximum equivalent stress of the optimized crankshaft model was reduced by 9.43%, maximum deformation was decreased by 3.68%, and the mass was reduced by 1.30%. The relationship between the frequency and the vibration modal was explained.

Low weight and high structural rigidity are important factors essential for all elements of an internal combustion (IC) engine. So, much research has been presented to optimize the proper material properties for a crankshaft. Modeling and optimization analysis of the crankshaft were performed to evaluate the fatigue performance of different types of materials such as forged steel, and ductile cast iron [18, 19]. A modified lightweight safe design was proposed using AISI 1045 which produced maximum von Mises stresses of 184.21 MPa, safety factor of 2.4428, and weight reduction of 4.04 % less if compared to the considered crankshaft model. FEA of the crankshaft with a 4-cylinder petrol engine of Maruti swift was carried out by ABAQUS software using six materials [20]. The optimized crankshaft was much stiffer than the C 70 Alloy material. It resulted in a 65.539% weight reduction. Modeling and analysis of a four-wheeler crankshaft with different aluminum alloys were presented [21]. This result illustrated that aluminum alloy 7475 was better than 6061 alloy and the thermal gradient value was higher. Experimental and analytical investigations of steel specimens with high surface quality were discussed [22, 23]. A new optimizing counterweight methodology was developed to reduce total mass [24].

In the v6 engine, six cylinders are connected to a common crankshaft in V-configuration. A v6 crankshaft is more compact, shorter and has higher speeds than inline engine crankshafts. Pistons usually have a smaller stroke, leading to

faster acceleration and lower operating temperature. The v6 crankshafts are commercially successful in mid-size cars because it is less expensive to build and consume less fuel than the v8. A high-strength marine diesel v-type engine crankshaft was analyzed [25]. It was detected that crankshaft fatigue strength may be maximized by larger fillet radius, web thickness and, web width. The effect of fillet radius and web thickness on crankshaft fatigue strength was higher than web width. From the above literature, most research discussed static failure analysis, fatigue analysis, design optimization, and material selection for inline engine crankshafts. Little work has been carried out for the v-type engine crankshafts. In this work, the v6-engine crankshaft is investigated to determine the optimum fillet radius that ensures minimum equivalent stresses and total deformation at the most critical area in the crankshaft.

2. Static analysis of v6-crankshaft

The objective of static analysis of the v6-crankshaft is to detect its operational behavior under mechanical loading to ensure operation safety. There are two different load sources in a crankshaft operation; inertia and combustion. The inertia of rotating components applies forces to the crankshaft which is directly related to the rotating speed and acceleration of rotating components. Gas combustion forces are transmitted to the crankshaft based only on the dimensions of the piston and connecting rod. These two load sources generate both bending and torsional loads on the crankshaft. Torsional load is usually ignored for the stress analysis of the crankshaft [6], as it is less than 10% of the bending load. In addition, when the peak of the bending load takes place, the magnitude of the torsional load is zero. Assuming a v6-crankshaft with a single crank throw, all stresses acting upon the crankshaft critical sections [25] can be calculated as illustrated in the following sections.

2.1. Normal stresses at crankshaft fillets

In v-type engine crankshafts, two radial forces are generated on each crankpin as there are two cylinders connected on the same crankpin, as

shown in Fig. 1. Normal stress due to bending moment is generated at each crankshaft phase. However, the main geometric parameters of the v6-crankshaft, which are used in many applications such as the Ford F-150 engine, are defined in Table 1.

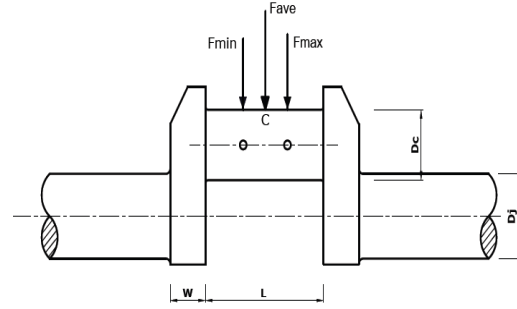


Fig. 1. Applied forces acting on v6-crankpin.

Table 1. Main geometric parameters of the v6-crankshaft model.

Parameter name	Parameter value (mm)
Length of the crankshaft, L_{cs}	564.88
Main journal diameter, d_j	63.5
Crankpin diameter, d_c	76.2
Length of the main journal, L_j	53.34
Length of the crankpin, L_c	54.62
Fillet radius of the crankpin, R_{CF}	0.64
Fillet radius of the main journal, R_{JF}	0.64
Web thickness, W	19.00
Web width, B	100.00

For maximum pressure, P_{max} , produced by gas combustion and the inertia, a maximum force F_{max} , will be generated and can be calculated by Eqs. (1) and (2).

$$F_{max} = P_{max} \cdot \frac{\pi d_c^2}{4} \quad (1)$$

$$F_{min} = P_{min} \cdot \frac{\pi d_c^2}{4} \quad (2)$$

For a crankpin, assume that an average force, F_{ave} , is acting at midpoint C, as shown in Fig. 1. Hence, nominal normal stress due to bending moment acting on the web cross-section, σ_{NB} , can be defined by Eqs. (3) and (4).

$$\sigma_{NB} = \pm \frac{6M_{ave}}{b w^2} \quad (3)$$

$$M_{ave} = \frac{F_{ave} \cdot L}{4} \quad (4)$$

where:

M_{ave} is the average equivalent bending moment acting at point C.

Nominal normal stress due to radial forces acting on the web cross-section, σ_{NR} , can be defined by Eq. (5).

$$\sigma_{NR} = \pm F_{eq}/A_{web} \quad (5)$$

where:

F_{eq} is the equivalent radial forces acting on the web cross-section; and A_{web} is the web cross-section area, $A_{web}=W \cdot B$

Stress concentration factors should be considered to calculate the effect of normal stresses at the critical sections of the crankshaft.

For the crankpin fillet, only normal stress, due to the bending moment, is presented by Eq. (6).

$$\sigma_{CF} = \pm(\alpha_1 \bullet \sigma_{NB}) \quad (6)$$

where:

σ_{CF} is the maximum normal stress in a crankpin fillet; and α_1 is the stress concentration factor for bending in a crankpin fillet.

For the journal fillet, normal stress, due to bending moment and radial force, is calculated by Eq. (7).

$$\sigma_{JF} = \pm(\beta_1 \bullet \sigma_{NB} + \beta_2 \bullet \sigma_{NR}) \quad (7)$$

where:

σ_{JF} is the maximum normal stress in the journal fillet; and β_1 and β_2 are the stress concentration factors in the journal fillet for bending and compression.

In addition to the maximum bending stresses in fillets, additional bending stresses, σ_{add} , due to misalignment, deformation, and vibrations should be considered.

2.2. Torsional stresses at crankshaft fillets.

Torsional stresses should be determined at the crankpin fillet as well as for the journal fillet.

For the crankpin fillet: nominal torsional stress acting on the crankpin cross-section, τ_C , can be calculated by Eqs. (8) and (9).

$$\tau_C = \frac{16 T}{\pi d_c^3} \quad (8)$$

$$\tau_{CF} = \pm(\alpha_T \bullet \tau_C) \quad (9)$$

where:

τ_{CF} is the maximum torsional stress in crankpin fillet; and α_T is the stress concentration factor for torsion in crankpin fillet.

For the journal fillet: nominal torsional stress acting on the journal cross-section, τ_J , can be calculated by Eqs. (10) and (11).

$$\tau_J = \frac{16 T}{\pi d_j^3} \quad (10)$$

$$\tau_{JF} = \pm(\beta_T \bullet \tau_J) \quad (11)$$

where:

τ_{JF} is the maximum torsional stress in the journal fillet; and β_T is the stress concentration factor for torsion in the journal fillet.

2.3. Equivalent von-mises stresses at the crankshaft fillets.

Bending and torsional stresses at the fillets generate a biaxial stress effect represented by Eqs. (12) and (13).

For the crankpin fillet:

$$\sigma_{vCF} = \pm \sqrt{(\sigma_{CF} + \sigma_{add})^2 + 3\tau_{CF}^2} \quad (12)$$

For the journal fillet:

$$\sigma_{vJF} = \pm \sqrt{(\sigma_{JF} + \sigma_{add})^2 + 3\tau_{JF}^2} \quad (13)$$

3. Modeling of v6-crankshaft and material selection

For accurate results during the simulation analysis, a 3d model of the v6-crankshaft has been carried out using SolidWorks software with geometric parameter values given in Table 1. The General specifications of the V-type engine are included in Table 2. Medium-carbon steel alloys, such as nickel-chrome-moly alloy SAE-4340 and AISI 1045, are commonly used for the manufacturing of crankshafts to ensure hardness, yield strength, fatigue strength, ductility, and other desired properties of the crankshaft. Forged steel, AISI 1045, is selected for this simulation with specifications given in Table 3.

Using these parameters, the generated model of the crankshaft in SolidWorks has been imported to the ANSYS workbench for further simulation study.

Table 2. V6-engine specifications [25].

Specifications	Value
No. of cylinders	6
Power	180 HP
Torque, T	238 N.m
Engine displacement	2.0 L
Top speed	107-176 mph
RPM, N	5400
Piston diameter, d_p	70 mm

Table 3. Mechanical properties of AISI 1045 forged steel.

Property	Value
Modulus of elasticity (GPa)	205
Poisson ratio	0.29
Ultimate tensile strength (MPa)	625
Yield stress (MPa)	530
Density (kg/m ³)	7850

3.1. Model finite element analysis

FEA has been used to detect the state of stresses at critical sections to optimize the life of the crankshaft. The proposed crankshaft model geometry is meshed with tetrahedral elements. Mesh refinement should be improved for critical locations such as crankpin fillet and journal fillet to enhance simulation results. The proposed mesh resulted in about 572383 elements with 365317 nodes. However, all analyses depend on the linear properties of the crankshaft material. The generated model mesh is shown in Fig. 2(a).

3.2. Model boundary conditions.

Boundary conditions are critical factors that control the accuracy of the simulation process. The boundary conditions in the ANSYS software model include the applied load on the crankpin neck surface and other constraints based on the crankshaft bearing configuration. Torsional load is usually ignored in the static analysis of the crankshaft. To formulate a crankshaft subjected to bending stress, the whole surface of each crankpin is a force of 50 kN produced from the kinematic analysis of the proposed v6-crankshaft. However, the crankshaft is expected to have fixed supports at the ends and cylindrical supports at the main journals, as shown in Fig. 2(b).

3.3. Model solution

The model solution has been carried out for equivalent von Mises stress, total deformation, axial deformation, and safety factor. The maximum stress value is 430.2 MPa at the journal fillet area, as shown in Fig. 3(a). However, similar lower stress values are located away from the fillet areas. Maximum total deformation is 0.14 mm at the web surface area, as shown in Fig. 3(b). Maximum axial deformation is 0.08 mm at the crankpin fillet, as shown in Fig. 3(c). Minimum safety factor is 1.338 at the journal fillet area, as shown in Fig. 3 (d).

4. Parametric optimization

From the previous solution, fillet areas are the most critical stress areas. So, optimum values of journal fillet radius and crankpin fillet radius ensure maximum crankshaft safety. To optimize these parameters, a parametric direct optimization tool has been used. All optimization parameters, initial values, constraints, and objectives are presented in Table 4. Optimization results are indicated in Table 5 for eight sample design points that meet the optimization constraints and objectives.

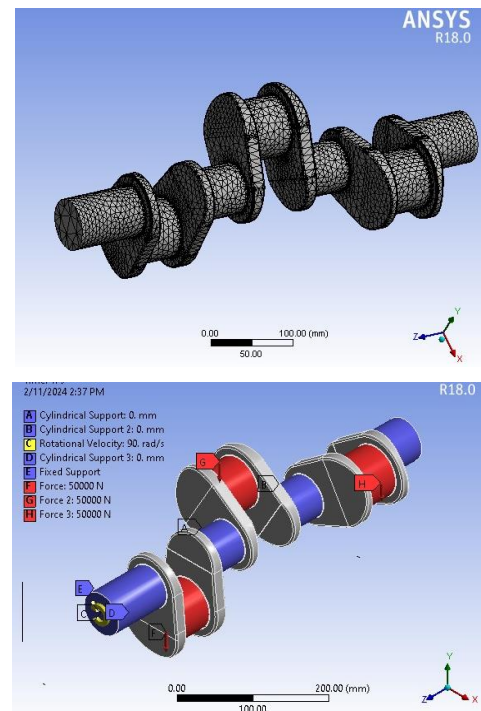


Fig. 2. (a) FEA model and (b) boundary conditions.

Table 4. Optimization parameters, constraints and objectives.

Input parameter	Initial value	Constraints	Output parameters	Objective
Crankpin fillet radius, R_{CF} (mm)	0.64	$0.5 \leq R_{CF} \leq 1.0$	Maximum equivalent stress	minimize
Main journal fillet radius, R_{JF} (mm)	0.64	$0.5 \leq R_{JF} \leq 1.5$	Maximum total deformation	minimize
Crankshaft mass, m (kg)	24.087	--	Crankshaft mass, m (kg)	minimize

Table 5. Optimization results for input and output parameters.

Sample design points	R_{JF} (mm), P1	R_{CF} (mm), P2	Mass (kg), P3	Maximum equivalent stress (MPa), P4	Maximum total deformation (mm), P5	Safety factor, P6
1	0.5625	0.53125	24.08669314	481.1051788	0.144379082	1.1966203
2	0.6875	0.78125	24.08781741	415.8406631	0.144214505	1.384425032
3	0.8125	0.65625	24.08776051	387.8292924	0.144206576	1.484416558
4	0.9375	0.90625	24.0891681	351.8447111	0.144014455	1.636233841
5*	1.0625	0.59375	24.08853087	329.4767403	0.144028252	1.747316738
6	1.1875	0.84375	24.08999093	317.3090301	0.143843003	1.814320327
7*	1.3125	0.71875	24.09015477	310.3313898	0.14382158	1.855114378
8*	1.4375	0.96875	24.09189964	281.9995004	0.143522339	2.04149377

* Candidate design points

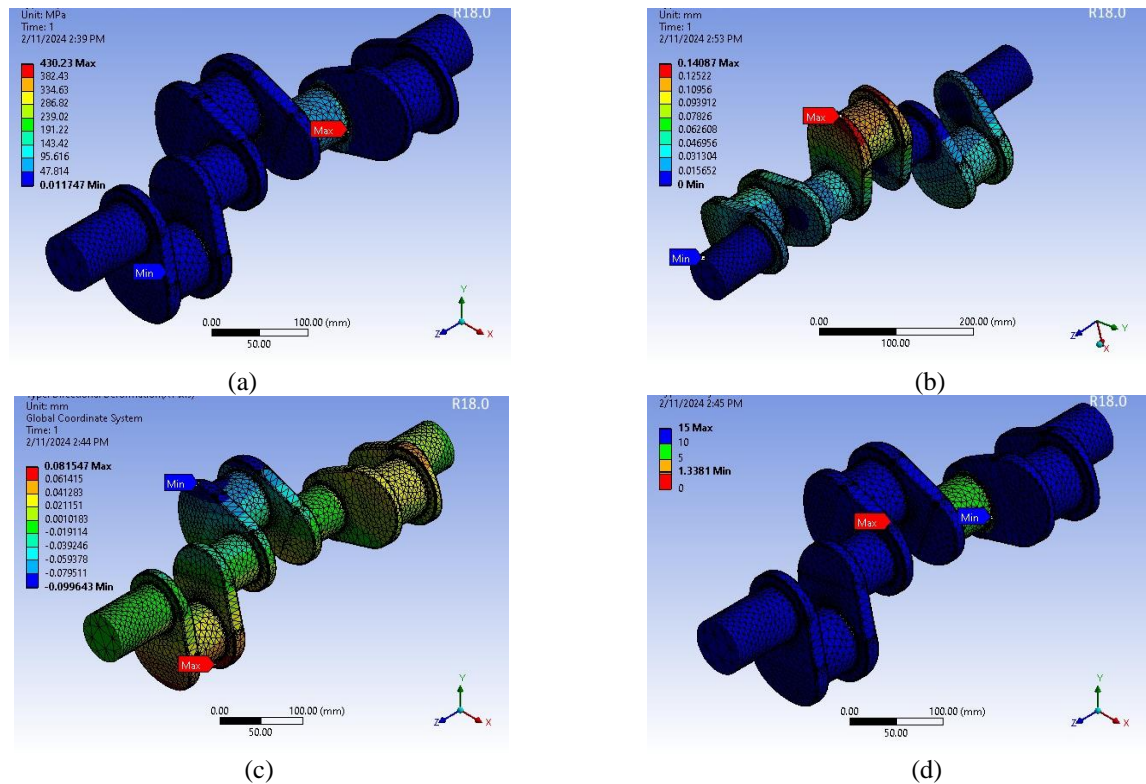


Fig. 3. Original model solutions: (a) Equivalent von-mises stress distribution, (b) Total deformation distribution, (c) Axial deformation distribution, and (d) Safety factor values distribution.

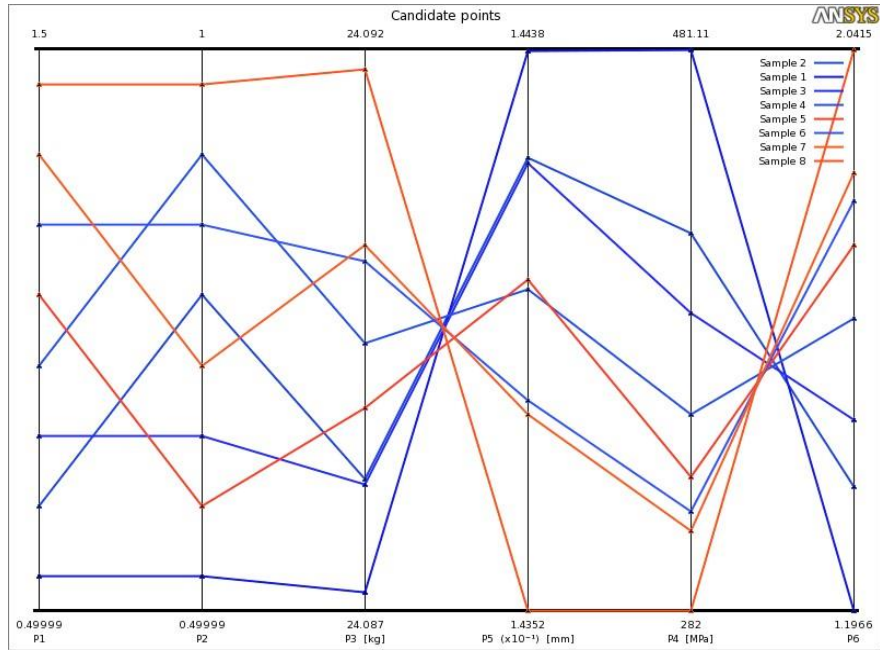


Fig. 4. Sample design points chart.

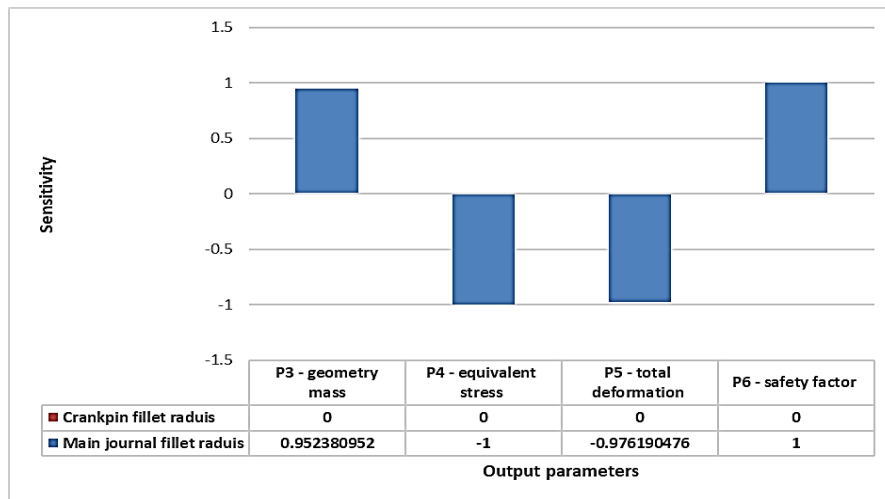


Fig. 5. Sensitivity analysis chart for output optimization parameters.

5. Results and discussion

From the above optimization results, it can be denoted that increasing the values of fillet radii causes an increase in crankshaft mass and safety factor. A corresponding decrease in von Mises equivalent stress and total deformation is observed, as illustrated in samples chart shown in Fig. 4. It is also denoted that the change in the main journal fillet radius has a noticeable effect on all output parameters.

In contrast, the crankpin fillet radius has no noticeable effect on these parameters, as illustrated in the sensitivity chart shown in Fig. 5. So, further analysis for the effect of change in fillet radius of the main journal on other optimization parameters has been carried out, as illustrated in Fig. 6. Generally, an increase in the main journal fillet radius is directly proportional to the crankshaft mass and corresponding safety factor. While an increase in the main journal fillet radius is inversely proportional to the maximum equivalent stress.

The optimization process produces the best three candidate design points, as indicated in Table 5. The candidate optimum points are compared with each other and with the original model state as shown in Table 6. It is shown that candidate point 8 is the most proper design point as it produces a suitable decrease in equivalent stress (34.45%) and minimum increase in total deformation (1.91%) with moderate mass

increase (0.02%) if compared to the original model given in Table 6.

5.1. Optimized model results

The optimum design point ‘8’ is applied to the model and all design parameters are recalculated. Then, the optimized model solution is generated for equivalent von Mises stress, total and axial deformation, and safety factor, as shown in Fig. 7.

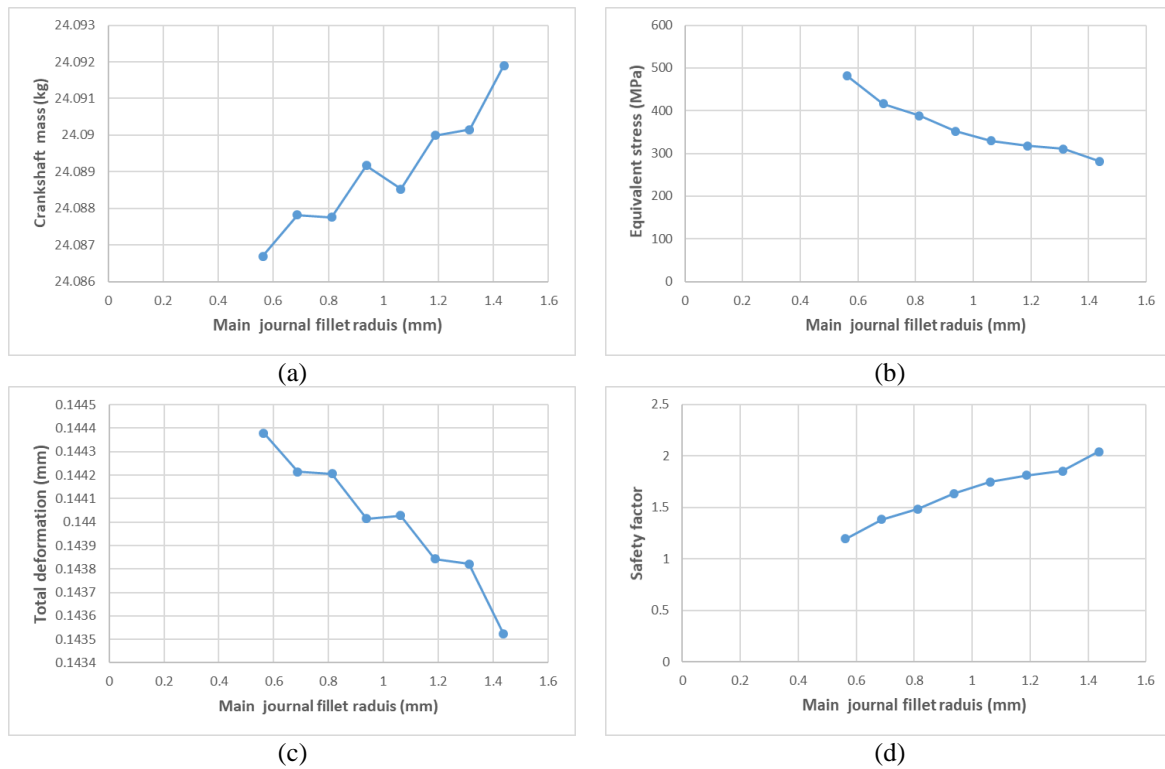


Fig. 6. Influence of main journal fillet radius on different design parameters: (a) influence of journal fillet radius on crankshaft mass, (b) influence of journal fillet radius on equivalent stress, (c) influence of journal

Table 6. Variation of output parameter values for proposed design points vs original model.

Proposed design point	R_{JF} (mm)	R_{CF} (mm)	P3 - Geometry mass (kg)		P4 - Equivalent stress (MPa)		P5 - Total deformation (mm)	
			Parameter value	Variation from reference%	Parameter value	Variation from reference%	Parameter value	Variation from reference%
Point 8*	1.437	0.968	24.091899	0.02	281.9995004	-34.45	0.143522339	1.91
Point 7	1.312	0.718	24.090154	0.012	310.3313898	-27.87	0.14382158	2.13
Point 5	1.062	0.593	24.088530	0.004	329.4767403	-23.4	0.144028252	2.27

* Optimum design point

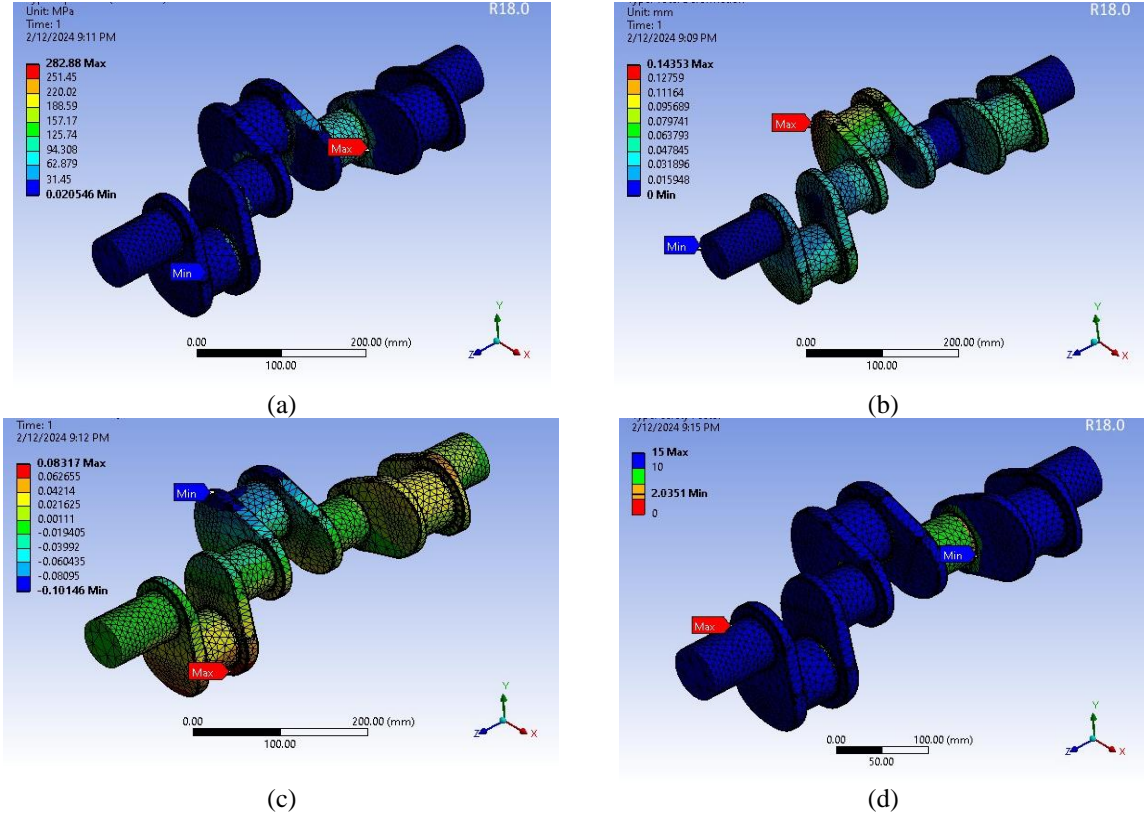


Fig. 7. Optimized model solutions: (a) equivalent von Mises stress distribution, (b) total deformation distribution, (c) axial deformation distribution, and (d) safety factor values distribution.

5.2. Optimized model validation

To validate the efficiency of the optimization process, the optimized model solution should be compared with the theoretical calculations and original model solution as illustrated in [Table 7](#).

Theoretical calculations are based on Eqs. (1-13). However, an increase of 124.6% and 54.36% in journal fillet radius and crankpin radius respectively generate an increase of 0.02% in crankshaft mass. It also generates a decrease of 32.6% in maximum von Mises equivalent stress, 7.2% in a safety factor, and a 6.2% decrease in total deformation. As compared with previous work, very little work has been found for the proposed type of v6 crankshaft. Another type of v6 crankshaft has been investigated [25]. However, common results are detected such as the effect of the main journal fillet radius on maximum equivalent stress.

6. Conclusions

A model for v6-crankshaft has been presented for static analysis. A simulation process, using ANSYS software, has been applied to evaluate the state of stresses at stress concentration areas, including finite element analysis, material, and boundary conditions identification. The model solution has been generated for maximum equivalent stress, total deformation, and safety factor. Geometric optimization has been developed to obtain the most proper values of the main journal and crankpin fillet radii with their corresponding values of maximum equivalent stress, total deformation, safety factor, and crankshaft mass. The study proved the main journal fillet radius has the greatest effect on the output parameters. The optimized model resulted in a 0.02% increase in crankshaft mass, a 34.45% decrease in maximum equivalent stress, and a 1.91% increase in total deformation. These results indicate more enhancement in v6-crankshaft performance.

Acknowledgments: The authors are grateful to Future University in Egypt (Cairo, Egypt) for providing all the required facilities to carry out the present research.

Declarations

Conflict of interest: The authors declare that they have no conflict of interest.

References

- [1] G. Çevik and R. Gürbüz, "Effect of Fillet Rolling Load on the Fatigue Performance of a Micro-Alloy Steel Diesel Engine Crankshaft", *IOP Conf. Series: J. Physics*, Vol. 843, (2017). <https://iopscience.iop.org/article/10.1088/1742-6596/843/1/012044>.
- [2] M. Cevik, H. Hochbein, and M. Rebbert, "Potentials of Crankshaft Fillet Rolling Process", *SAE Int. J. Engines*, Vol. 5, No. 2, (2012). <https://doi.org/10.4271/2012-01-0755>.
- [3] W. Chien, J. Pan, D. Close, S. Ho, "Fatigue analysis of crankshaft sections under bending with consideration of residual stresses", *Int. J. Fatigue*, Vol. 27, pp.1-19, (2005). <https://doi.org/10.1016/j.ijfatigue.2004.06.009>.
- [4] K. Choi, J. Pan, "Simulations of stress distributions in crankshaft sections under fillet rolling and bending fatigue tests", *Int. J. Fatigue*, Vol. 31, pp. 544–557, (2009). <https://doi.org/10.1016/j.ijfatigue.2008.03.035>.
- [5] J. Sun, X. Liu, X. Hu, J. Zhang, P. Cui, "Simulation for Crankshaft Fillet Mechanical Impact Process", *IOP Conf. Series: Earth, Env. Sci.*, Vol. 252, (2019). <https://doi.org/10.1088/1755-1315/252/2/022098>.
- [6] H. Montazersadgh and A. Fatemi, "Dynamic Load and Stress Analysis of a Crankshaft", *SAE Tech. paper series*, Vol. 01, No. 0258, (2007). <https://doi.org/10.4271/2007-01-0258>.
- [7] F. Liu, Z. Zheng, D. Han, Y. Zhang, "Finite element analysis of a vehicle diesel engine crankshaft", *IOP Pub. Conf. Series: J. Physics*, Vol. 1653, (2020). <https://doi.org/10.1088/1742-6596/1653/1/012042>.
- [8] M. Degefe, P. Paramasivam, T.Dabasa, V. Kumar, "Optimization and finite element analysis of single cylinder engine crankshaft for improving fatigue life", *American J. Mech., mat. Eng.*, Vol. 1, No. 3, pp.58-68, (2017). [doi:10.11648/j.ajmme.20170104.12](https://doi.org/10.11648/j.ajmme.20170104.12).
- [9] J. Zhu, G. Wang, S. Jia and W. Gao, "Fatigue analysis of marine diesel engine crankshaft", *IOP Pub. Conf. Series: J. Physics*: Vol. 2336, (2022). <https://doi.org/10.1088/1742-6596/2336/1/012006>.
- [10] X. Chen, X. Yu, R. Hu, J. Li, "Statistical distribution of crankshaft fatigue: experimental. and modeling", *Eng. Failure Ana.*, Vol. 42, pp: 210–22, (2014). <https://doi.org/10.1016/j.engfailanal.2014.04.015>.
- [11] H. Bayrakc, S. Tasgetiren, F. Aksoy, "Failures of single cylinder diesel engines crank shafts", *Eng. Failure Ana.*, Vol. 14, pp.725–73, (2007). <https://doi.org/10.1016/j.engfailanal.2006.01.006>.
- [12] M. Fonte, V. Infante, L. Reis, M. Freitas, "Failure mode analysis of a diesel motor crankshaft", *Eng. Failure Ana.*, Vol. 82, pp.681–686, (2017). <https://doi.org/10.1016/j.engfailanal.2017.06.010>.
- [13] Ö. CİHAN, "Deformation and stress analysis of crankshafts for single cylinder and four cylinder ic engine using ansys", *Cumhuriyet Sci. J.*, Vol. 41, No. 1, pp. 298-304, (2020). <https://doi.org/10.17776/csj.586687>.
- [14] A. Dindore, G. Badiger, "Optimization of crankshaft by modification in design and material", *Int. Res. J. Eng. and Tech. (IRJET)*, Vol. 07, No. 03, (2020). <https://www.irjet.net/archives/V7/i3/IRJE-T-V7I3668.pdf>.
- [15] Y. Zuan, P. Xuan, "Study on Failure Analysis of Crankshaft Using Finite Element Analysis", *MATEC Web of Conf.*, Vol. 335, (2021). <https://doi.org/10.1051/mateconf/202133503001>.
- [16] B. Zheng, J. Zhang, J. Lei, "Crankshaft Optimization Based on Experimental Design and Response Surface Method"

- Math. Prob. in Eng.*”, *Hindawi*, Vol. 2022, (2022).
<https://doi.org/10.1155/2022/9286969>.
- [17] R. Deshbhratar, Y. Suple, “Analysis & Optimization of Crankshaft Using Fem”, *Int. J. Modern Eng. Res. (IJMER)*, Vol. 2, No. 5, pp.3086-3088, (2012).
https://www.ijmer.com/papers/Vol2_Issue 5/U02530863088.pdf.
- [18] C.M. Balamurugan, R. Krishnaraj, M. Sakthivel, K.Kanthavel, D. Marudachalam, R.Palani, “Computer Aided Modeling and Optimization of Crankshaft”, *Int. J. Sci. & Eng. Res.*, Vol. 2, No. 8, (2011).
<https://www.ijser.org/researchpaper/computer-aided-modeling-and-optimization-of-crankshaft.pdf>.
- [19] A. Pandiyan, A. Kumar, G. Patel and S. Asif, “Design and Optimization of Crankshaft for Single Cylinder 4 – Stroke Spark Ignition Engine Using Coupled Steady-State Thermal Structural Analysis”, *Int. J. Mech. Eng. Tech.*, Vol. 9, No. 7, pp. 135–145 (2018).
<http://www.iaeme.com/IJMET/issues.asp?JType=IJMET&VType=9&IType=7>.
- [20] B. Ganesh, Z. Bhaskar, P. Amol, “Design, optimization and finite element analysis of crankshaft”, *Int. J. Inn. Eng. Res. Tech., [IJIERT] ICITDCEME’15 Conf. Proc.*, Vol. 15, (2018).
https://www.academia.edu/78084882/Design_Optimization_and_Finite_Element_Analysis_of_Crankshaft.
- [21] A. Sandeep, M. John, S.P. Jani, “Theoretical modelling and analysis of a four-wheeler crank shaft by different aluminum alloys”, *Mat. Tod.: Pro.*, Vol. 45, pp. 1679–1683, (2021).
<https://doi.org/10.1016/j.matpr.2020.08.560>.
- [22] H Hatami, “Experimental and analytical investigation of bending and impact properties of steel composite beams with high performance concrete”, *Journal of Solid and Fluid Mechanics*, Vol. 12, No. 6, pp: 99-111 (2023).
[10.22044/JSFM.2023.12514.3680](https://doi.org/10.22044/JSFM.2023.12514.3680)
- [23] M Khazali, H Hatami, “An Experimental Investigation on the Effects of MQL Method on Grinding of Nickel Based Superalloy 738 (Inconel 738)”, *Journal of Modeling in Engineering*, Vol. 21, No. 74, pp. 125-151 (2023).
<https://doi.org/10.22075/jme.2023.24361.2136>
- [24] Eugenio Brusa, Alberto Dagna , Cristiana Delprete, Chiara Gastaldi, “A two-step optimization for crankshaft counterweights”, *Engineering Science and Technology, an International Journal*, Vol. 51, (2024).
<https://doi.org/10.1016/j.jestch.2024.101657>.
- [25] S. Jia, G. Wang and J. Zhu, “Fatigue strength analysis of crankshaft based on rules for classification of sea-going steel ships”, *IOP Pub. Conf. Series: J. Physics: Vol. 2336*, (2022).
<https://doi.org/10.1088/1742-6596/2336/1/012004>

